Applied Thermal Engineering 248 (2024) 123195

Contents lists available at ScienceDirect

Applied Thermal Engineering

journal homepage: www.elsevier.com/locate/apthermeng

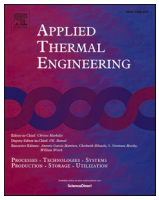

Research Paper

Energy modeling, calibration, and validation of a small-scale greenhouse using TRNSYS

Arnaud Beaulac [a], Timothé Lalonde [b], Didier Haillot [a], Danielle Monfet [a,*]

[a] École de Technologie Supérieure, Montreal, Quebec, Canada
[b] Ferme d'Hiver Technologies, Brossard, Quebec, Canada

ARTICLE INFO

Keywords:
Greenhouse energy model
TRNSYS
Sensitivity analysis
Calibration
Validation
Building performance simulation

ABSTRACT

Greenhouse energy modeling is a prevalent tool for optimizing greenhouse energy consumption. However, for a model to serve its intended use, it is imperative to have a high level of confidence in the precision of its predictions. In this paper, a validated greenhouse energy model for a typical small-scale greenhouse in a cold climate is developed. The model is created using TRNSYS, a building performance simulation tool, with detailed energy modeling components and a user-defined crop model. The model is calibrated to fix uncertain parameters. A sensitivity analysis is used first to identify sensible uncertain parameters, followed by a multi-stage automated calibration. The automated calibration method uses a multi-objective genetic algorithm to adjust the uncertain parameters, calibrating the model for the measured indoor air temperature and relative humidity. The model performed well during the free-floating and ventilated stages (56 days) with a combined root mean square error (RMSE) of 1.6 °C for indoor air temperature and 8.3 % for the air relative humidity. The validation process involved assessing the applicability of the calibrated model using two additional datasets. For all the cases, comparing the simulation results with indoor environment measurements resulted in an RMSE of less than 2 °C for air temperature and less than 10 % for air relative humidity; these values compare favorably to the literature. The model achieved a 3.7 % mean relative error (MRE) in estimating monthly energy consumption for a minimally heated greenhouse. Given these results, the model is deemed sufficiently accurate and applicable for future investigations.

1. Introduction

Recently, a rising interest in year-round local food production solutions has emerged. Greenhouses effectively control indoor environment conditions to optimize crop growth. In cold climates, the economic viability of greenhouses is directly linked to the expenses associated with the energy required for cultivating crops under optimal conditions [1,2]. Building performance simulation (BPS) can generate high-quality data to improve energy efficiency without the time and investments associated with conducting real-life experiments. Dynamic greenhouse energy models can assist in decision-making regarding indoor environment management, crop cultivation, greenhouse design, energy conservation measures (EMC), investments, and policymaking [3–6]. Different modeling approaches have been proposed, such as using process-based greenhouse models. Process-based models explicitly simulate the phenomena and systems by underlying processes and mechanisms that drive the system's behavior, such as the crop's physiological processes and the energy balance within the greenhouse. Thus, process-based models are known for their high interpretability and often exhibit high accuracy [7].

Many process-based greenhouse energy models are developed using BPS tools like TRNSYS [8]. Between 2013 and 2023, at least thirty-two studies have used TRNSYS to create a greenhouse energy model [9]. TRNSYS has been effectively used to consider design features accurately across multiple types of greenhouses. The models yield acceptable results when greenhouse-specific elements are added [10]. Indeed, TRNSYS supports implementing simplified and detailed modeling approaches for thermal processes, such as 3D solar and thermal radiations, ground-coupling (Type 49/1244), and infiltration/ventilation (TRNFLOW). Additional components can be integrated into TRNSYS to address greenhouse-specific elements to model additional phenomena, such as crops' evapotranspiration and condensation on the greenhouse

* Corresponding author at: École de technologie supérieure, Department of Construction Engineering, 1100, rue Notre-Dame Ouest, Montreal, Quebec H3C 1K3, Canada.
E-mail address: danielle.monfet@etsmtl.ca (D. Monfet).

https://doi.org/10.1016/j.applthermaleng.2024.123195
Received 14 December 2023; Received in revised form 4 April 2024; Accepted 15 April 2024
Available online 19 April 2024

structure [11,12]. Although these components have been integrated individually in published TRNSYS models, none have combined all the detailed components simultaneously in one model [9].

Despite the numerous recent models, direct comparisons of model performance solely based on validation results have become challenging, given the wide range of evaluation techniques. As Katzin et al. [7] and Beaulac et al. [9] noted, there are no standardized procedures for validating greenhouse energy models. Validation processes vary in terms of both data acquisition characteristics (validated variables, duration of the validation periods, sampling frequency, etc.) and metrics used.

Validation is essential in developing the greenhouse energy model, as it instills confidence in its accuracy. However, greenhouse model validations are often limited. They frequently involve short-term assessments using hourly data or extended validation periods with a longer sampling frequency (e.g., monthly). This can result in an inadequate representation of all operating modes [13]. Given the sensitivity of greenhouses' thermal behavior to outdoor weather conditions, comprehensive validation across diverse meteorological conditions is essential to enhance confidence in the model's ability to estimate the annual energy performance of the greenhouse.

Validation poses additional challenges when dealing with process-based models, as they involve many parameters that depend on the level of detail in describing physical interactions. Parametrization, which consists of assigning values to these model parameters, typically draws from similar studies in scientific literature, established norms, standards, or field surveys. The values assigned to parameters may not faithfully represent their real-world counterparts due to the specific conditions under which they were initially determined. As a consequence, these values are regarded as possessing inherent uncertainty. Uncertain parameters can be calibrated by fitting the model's estimated values with the measured data. Calibration helps fix uncertain parameters of a greenhouse energy model to better represent the as-built and actual operating conditions, thereby enhancing accuracy.

Calibration can be either manual or automated. Manual calibration typically requires iterative tuning of individual parameters and is time-consuming, whereas automated data-driven calibration supports tuning multiple parameters simultaneously [14]. In recent years, with the increased computational capabilities, automated calibration has gained popularity within the building energy simulation field due to its robustness, leading to a shift in calibration methods from manual to automated [15]. The automated calibration uses an optimization algorithm to minimize the difference between measured and simulated data. Automated procedures often include sensitivity analysis to reduce the number of inputs before applying an optimization algorithm to reduce the computing time.

In greenhouse energy modeling, calibration is often manual, and the process is rarely described, thus replicable. Some of the reviewed TRNSYS models mentioned a calibration process [16–20], but it usually compared modeling approaches. For example, Rasheed et al. [19] assessed the impact of the tilted surface radiation models available in TRNSYS on validation metrics. Other greenhouse energy models used automated calibration, employing various optimization algorithms. Particle swarm optimization (PSO) has been used by [21–25], genetic algorithms (GA) by [21,26,27], and differential evolution (DE) algorithm by [24]. Another hybrid approach combined optimization and machine learning algorithms [4]. Chen et al. [21] compared GA and PSO with a novel hybrid approach combining adaptive PSO and GA (APSO-GA). The APSO-GA saved approximately 15 % of the optimization time and improved power and energy demand prediction accuracy by ~3 % compared to PSO and GA over a 3-day period. Guzmán-Cruz et al. [28] compared three global evolutionary algorithms (GAs, Evolution Strategy (ES) and Evolution Programming (EP)) and two local search methods (Least Squares (LSQ) and Sequential Quadratic Programming (SQP)). Based on the information presented in [28], the EP algorithm outperformed the others in predicting temperature and relative humidity over 7 days. The estimation of relative humidity by LSQ and SQP proved less accurate, possibly influenced by local minima. While comparing the performance of different calibration methods is informative, it is essential to highlight that it is difficult to assess their reliability without standardized validation methods.

Despite the extensive body of research on greenhouse energy modeling, the above review highlights several key findings:

1- Only a limited number of TRNSYS models included detailed modeling approaches for each greenhouse component.
2- Using extensive validation processes, such as over extended periods with sub-hourly data, is not widely explored.
3- Most TRNSYS models relied on uncertain parameters either fixed according to the literature or adjusted using manual calibration methods: automated calibration for detailed greenhouse models has not been thoroughly studied.

This study aims to provide accurate predictions of the indoor environment conditions and energy consumption of a small-scale greenhouse in a cold climate. To attain this objective, a small-scale greenhouse energy model is developed using the BPS tool TRNSYS. This is completed according to the following three steps. First, the studied greenhouse is modeled in TRNSYS using detailed modeling approaches and user-defined components. Second, a multi-stage automated calibration is used to fix uncertain parameters of the initial model under different operating modes. Third, the calibrated model undergoes validation using two periods to demonstrate its applicability. A validated process-based model developed in TRNSYS offers maximum flexibility to support research across multiple disciplines, including agronomy, economics, energy, greenhouse design, etc.

This paper is organized as follows: Section 2 presents the methodology to create the greenhouse BPS model; Section 3 details the energy modeling approach used in TRNSYS; Section 4 presents the calibration process; and Section 5 shows the results of the calibration and validation. A discussion follows in Section 6.

2. Methods

This paper presents the creation process of a greenhouse energy model that is calibrated and validated using measured data. Measured data are monitored at two identical gothic arch greenhouses. Each greenhouse has a footprint of 250 m^2 (10.7 m × 23.2 m), is oriented 40° to the Northeast, and is located in Victoriaville, Canada (Fig. 1).

The main steps of model development are illustrated in Fig. 2 and include: (1) creation of the greenhouse energy model using a BPS tool, (2) automated calibration of the model's uncertain parameters, and (3) validation of the calibrated model.

2.1. Creation of the greenhouse energy model

The model is developed using TRNSYS18 [8]. It is chosen based on (1) its ability to implement new models, such as a detailed crop model [29]; (2) its ease in enabling the implementation of detailed modeling approaches for solar radiation, thermal radiation, infiltration, ventilation, and conduction in the ground; and (3) its previous application to BPS of greenhouses by several authors [9]. The modeling of solar radiation and thermal exchanges considers the 3D shape of the greenhouse. For the ground-coupling model, a 3D ground discretization model is available. For infiltration and ventilation, an air network model, TRNFLOW, is integrated into the 3D construction [30]. Detailed models are preferred since they enable a finer resolution analysis of building energy performance, requiring fewer assumptions [31]. The greenhouse model is created according to data sourced from construction documents, manufacturer's manuals, operator interviews, field surveys, field experiments, and ongoing field measurements, as detailed in Section 3.

Fig. 1. Monitored gothic arch greenhouses.

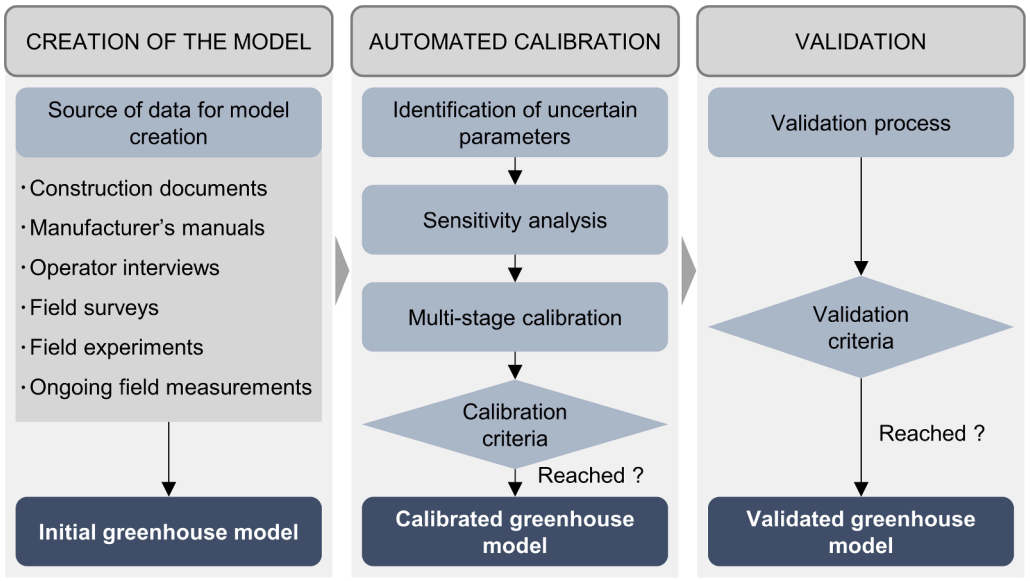

Fig. 2. Flowchart of the greenhouse energy model creation process.

2.2. Automated calibration

The automated calibration of uncertain parameters follows the approach proposed by Baba et al. [32]. Although initially designed for assessing overheating in commercial buildings, it is particularly relevant to greenhouses since they are prone to significant deviations from temperature setpoint due to being highly weather-dependent. Such temperature volatility can result in crops fatally overheating or freezing [33].

The calibration process includes: (1) identifying the uncertain parameters; (2) conducting a sensitivity analysis to reduce the number of uncertain parameters to be used in the multi-stage calibration by fixing insensitive parameters, i.e., parameters that do not significantly affect the indoor environment conditions of the greenhouse; (3) conducting a multi-stage calibration.

2.2.1. Identification of uncertain parameters

A detailed TRNSYS greenhouse model contains numerous parameters from mathematical expressions of thermal processes. To identify which parameters should be included in the calibration process and which should be fixed, a selection of uncertain parameters must be done. The first screening of parameters relies on expert knowledge since it is evidence-based. The screening process follows three steps to identify the uncertain parameters of the model.

First, all physicochemical properties of materials, heat transfer coefficient, and operating parameters used in the greenhouse model are listed. Modeling approaches and construction specifications are considered as modeling development elements rather than parameters. Also, the construction specifications are based on documentation and are confirmed with a field survey. Second, the parameters are categorized using an adapted version of the source hierarchy outlined by [31]: (1) Common knowledge; (2) Data-logged measurements; (3) Spot measurements; (4) Benchmark studies, standards, guidelines, and design stage information. Categories 1 and 2 are regarded as having a lower level of uncertainty; thus, the parameters in these categories are fixed to documented values. On the other hand, the more uncertain parameters (categories 3 and 4) are proceeded to the next step. Third, the remaining parameters are clustered according to two conditions: (1) the parameters can be consolidated into a single parameter (e.g., $\alpha = \frac{\lambda}{\rho^s Cp}$), and (2) the parameters are mathematically correlated (e.g., $\tau + \sigma + \rho = 1$). Finally, the remaining parameters are identified as the uncertain parameters of the greenhouse model.

2.2.2. Sensitivity analysis

Sensitivity analysis helps identify which input parameters significantly impact the output variables and which parameters are less sensitive. It can be fixed in the model without affecting the accuracy [34]. The proposed approach aims to reduce the number of parameters adjusted during calibration. The identification of sensible uncertain parameters is completed using the global variance-based sensitivity

method (SOBOL) [35], which can estimate the interactions between the parameters and is widely used in building energy analysis [15]. Calculated using the Monte Carlo method, it decomposes the variance of the model output into fractions attributable to individual inputs [35]. The global sensitivity index (S_{Ti}) of individual parameters calculates the contribution of each input parameter and its interactions with any of the other input parameters on the output for nonlinear and non-monotonic models, as shown in equation (1) [34].

$$S_{Ti} = 1 - \frac{V_{X\sim i}}{V(Y)} \tag{1}$$

where $V_{X\sim i}$ indicates the effect of all parameters except X_i on the model output, and $V(Y)$ is the total variance of the model output (variance of all parameters with all interactions).

Samples are generated using the Saltelli sampler from the Python library SALib [36]. The sum of the global sensitivity indices will be equal to 1 when the model is purely additive, as there is no correlation among the inputs. The number of samples is considered sufficient if the sum of the global sensitivity indices is equal to 1, and if not, the number of samples needs to be increased. The parameter range influences the application of the SOBOL method. A uniform distribution is assumed for each parameter.

2.2.3. Multi-stage calibration

Calibration settings are crucial to identify the optimal solution. Three essential elements of the calibration process are described in this section: the optimization algorithm selected for altering model parameters, the objective functions and evaluation criteria, and the calibration periods.

2.2.3.1. Multi-objective genetic algorithm. One of the evolutionary algorithms commonly used to generate high-quality solutions to optimization problems is a Genetic Algorithm (GA), as discussed by Chong et al. [15]. GA emulates the process of natural selection to evolve and improve a population of potential solutions across successive generations. Among the GAs, the Multi-Objective Genetic Algorithm NSGA-II (MOGA) optimization method is used. Multi-objective evolutionary algorithms are designed to find a set of solutions that represent the Pareto front. This front encompasses trade-off solutions that address multiple conflicting objectives simultaneously.

Calibrating greenhouses is challenging due to the interdependence of two main variables, air temperature and humidity, which influence indoor environment performance. Given this interdependence, simultaneous air temperature and humidity calibration are more appropriate than a single-objective approach. Hence, the MOGA calibration method is more suitable than the single-objective GA calibration. The Matlab function *gamultiobj* is used to apply the MOGA approach. A Matlab script is used to allocate the TRNSYS model code, specify the uncertain parameter ranges, and configure the MOGA settings to compute the objective functions. To configure the MOGA settings, Baba et al. [32] suggested a population size of 10 individuals to ensure diversity in novel solutions, with a maximum limit of 200 generations. The optimal solution is deemed reached when there is no change in any Pareto solutions for five consecutive generations. The simulations are conducted on an AMD Ryzen 9 7950X 16-Core Processor 4.5 GHz with 128 GB RAM.

2.2.3.2. Objective functions and selection criteria. As Katzin et al. [7] highlighted, there is no universally accepted statistical metric for evaluating greenhouse models. Each metric has its strengths and weaknesses. Therefore, using a combination of multiple metrics can offer a more comprehensive understanding of the performance of the model. Three metrics have been proposed as objective functions by Baba et al. [32]: Maximum Absolute Difference (MAD), Normalized mean Bias Error (NMBE), and Root Mean Square Error (RMSE) as defined by equations (2), (3) and (4). Each objective function will be computed separately for air temperature and humidity. Hourly metrics are used and calculated using the average of each timestep value over the last hour. This approach reduces the quantity of computed values while magnifying the impact of significant deviations. Normalized and relative metrics have been excluded from consideration due to their sensitivity to the average temperature, which exhibits substantial variability in an unheated greenhouse [7]. Furthermore, in an unheated greenhouse characterized by high daytime temperatures and cooler nights, the optimization of NMBE tends not to match daily temperature extremes, with lower daytime temperatures and higher nighttime temperatures. Therefore, instead of NMBE, the Mean Absolute Error (MAE) is used (5).

$$MAD = Max(|\hat{y}_i - y_i|) \tag{2}$$

$$NMBE = \frac{\sum_{i=1}^{n}(\hat{y}_i - y_i)}{n \cdot \bar{y}} \tag{3}$$

$$RMSE = \frac{\sqrt{\sum_{i=1}^{n}(\hat{y}_i - y_i)}}{n} \tag{4}$$

$$MAE = \frac{\sum_{i=1}^{n}|\hat{y}_i - y_i|}{n} \tag{5}$$

where $\hat{y}_i$ is the measured value and y_i the simulation value for each hour i.

As stated in Section 2.2.3.1, MOGA yields different Pareto front solutions, not necessarily converging a single solution that satisfies all objectives. Therefore, the 1 °C Percentage Error criterion is used to identify the Final Optimum Solution (FOS). The 1 °C Percentage Error criterion calculates the percentage of hours where the error between the simulated and measured indoor air temperature exceeds 1 °C over the calibration period. It is worth noting that the indoor temperature is the variable used for the FOS selection. It is a key performance metric in greenhouse energy simulation because of its direct relationship to heating consumption. For informational purposes, a 2 °C percentage error for indoor air temperature, a 5 % percentage error, and a 10 % percentage error for relative humidity are also evaluated.

Interior radiation measurements are omitted as calibration variables due to significant discrepancies in the measurements. The small shadows cast by opaque structural elements impact the measured radiation levels at different locations within the greenhouse. Indeed, relying solely on a single radiation meter inside the greenhouse does not provide a comprehensive understanding of the overall solar radiation transmission throughout the greenhouse.

2.2.3.3. Calibration periods. Analyzing measured datasets and establishing calibration periods are crucial to calibrating building models [13]. Chong et al. [15] reported that calibrating data from a building under free-floating conditions is a significant aspect of multi-stage approaches. This is because the number of uncertain parameters is reduced when there are minimal or no internal loads, such as occupancy, and when the HVAC system is not operating.

In the greenhouse, actual free-floating conditions are seldom for extended periods due to positive pressure fans for morning dehumidification, heating, and thermal blankets to cover and protect the cultivated crops. However, the vents are kept closed for extended periods to prevent frost damage. As a result, the calibration is completed in three stages using data collected over three distinct periods (Table 1). Notably, no calibration is undertaken during the colder months because of the ongoing use of thermal blankets to cover and protect the cultivated crops. The three calibration stages are used to calibrate different sets of parameters.

The first stage is used to calibrate sensible parameters, excluding the natural ventilation parameters. Natural ventilation plays a significant role in the energy balance. It is characterized by considerable uncertainty, primarily because it heavily depends on wind conditions, which

Table 1
Detail of each of the calibration stages.

Calibration stage	Description	Dates	Duration	Measured user-imposed inputs
1	Closed vents greenhouse	November 8th to 15th 2022 March 5th to 12th 2023	2 x 7 days	Fan actuators
2	Ventilated greenhouse	October 10th to 31th 2022	21 days	Fan actuators, Vents actuators
3	Ventilated greenhouse with modeled control	September 19th to October 10th 2022	21 days	

vary considerably over the data acquisition interval [37]. Ideally, mechanical ventilation would also be turned off, but this is impossible due to ongoing greenhouse operations. Mechanical ventilation uses positive pressure fans, and their operating status is set as an input to the model. Thus, this first phase of calibration is not influenced by errors in modeling the control sequence.

The second stage is used to calibrate the natural ventilation parameters, and all the other parameters are set to values obtained during the first calibration stage. The operating status of the vents and fans is imposed as inputs to the model for each timestep.

Finally, during the third stage of calibration, the control sequence is implemented in TRNSYS. This step confirms the calibration of the model, as the parameter values have already been calibrated.

2.3. Validation of the calibrated model

Once the greenhouse model is calibrated, the validation is carried out during a distinct period to ensure that the calibrated parameters perform effectively under different weather and operating conditions. Table 2 presents the validation periods.

First, the calibrated model will be assessed using data from the previous year (September and October 2021) for the same greenhouse. This serves as a validation of the calibration results and quantifies the impact of structural degradation. Second, the calibrated model is tested using data from an adjacent twin greenhouse. The twin greenhouse is minimally heated during winter using a propane air heater with a capacity of 44 kW and an estimated efficiency of 58 %. The heating is considered a ventilation heat gain to the greenhouse airnode, delayed by one-timestep (5 min) interval to account for air circulation and the location of the temperature sensor. The temperature, humidity, and heating consumption are validated using data gathered throughout an entire harvest period (October 2022 to March 2023).

Since heating consumption is an absolute scale unit, it can be evaluated against ASHRAE Guideline 14-2014 [38] criteria, which recommends a monthly CV-RMSE (Eq. (6)) under 15 % and NMBE (Eq. (7)) under 5 % for accurate models prediction.

Table 2
Validation periods of the calibrated model.

Validation period	Description	Dates	Duration	Validated variables
1	Unheated greenhouse using the previous year's data	September 18th to November 1st 2021	43 days	Indoor air temperature and relative humidity
2	Heated twin greenhouse	October 1st 2022 to March 1st 2023	162 days	Indoor air temperature and relative humidity, Heating consumption

$$CV(RMSE)(\%) = \frac{100}{\bar{y}_i}\sqrt{\frac{\sum_{i=1}^{n}(\hat{y}_i - y_i)^2}{n}} \quad (6)$$

$$NMBE(\%) = \frac{100}{\bar{y}}\frac{\sum_{i=1}^{n}(\hat{y}_i - y_i)}{n} \quad (7)$$

where $\bar{y}$ is the average measured value over the studied period.

3. Description of the greenhouse energy model

The greenhouse depicted in Fig. 1 features an envelope composed of double-layer polyethylene inflated films with the end walls being made of 6 mm clear polycarbonate panels. The greenhouse structure is made of 5 cm steel braces, resulting in a disposition such that the glazed surface of the envelope is about 93 % of the total surface. The greenhouse floor is covered with bare soil for cultivation.

The greenhouse is cooled by natural and forced ventilation using side vents, and two independently controlled 2.03 $m^3 \cdot s^{-1}$ positive pressure fans. The side vents are located 1 m above the ground and are 22 m long by 1 m high. They open gradually when the indoor temperature rises above the cooling set point. The first fan starts when the indoor temperature is above 15 °C and the second one if the indoor temperature is above 20 °C. The side vents are shut closed for temperatures below the freezing point. Additionally, four air circulation fans are used to continuously mix the air in the greenhouse, each having a flow rate of 0.7 $m^3 \cdot s^{-1}$ and dissipating 30 W of heat. Fig. 3 illustrates an overview of the greenhouse equipment. Additionally, the twin greenhouse shown in Fig. 1 is equipped with a propane air heater with a rated capacity of 44 kW.

3.1. Measured data

The twin greenhouses are fully instrumented to monitor the on-site weather conditions and indoor environment conditions. A weather station is installed nearby, about 100 m away. Weather data listed in Table 3 are recorded and used as inputs to the greenhouse model. Additional information, such as cloud cover, is gathered from nearby meteorological station datasets.

Indoor environment conditions are monitored using a Hobonet Remote Monitoring Station at 5-minute intervals. Details regarding the sensors, including their types and locations, are provided in Table 4. This instrumentation setup remains consistent across all datasets in the study.

Data are recorded year-round, but in the greenhouses under study, which are dedicated to research, cultivation only occurs during the colder months, from September to March. The greenhouses are primarily used for harvesting leafy green vegetables. The crop growth stage and sizes are based on monitoring conducted by the greenhouse operators. During the summer months, the greenhouses undergo a green

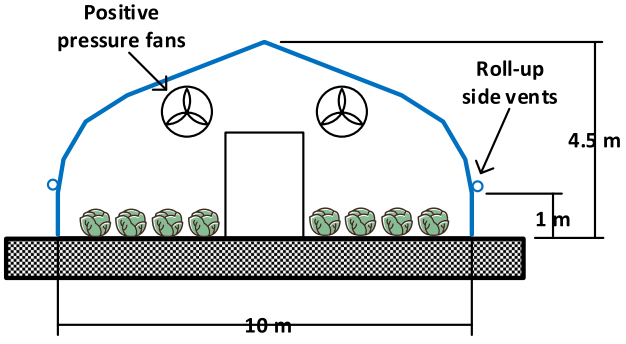

Fig. 3. Overview of the gothic arch greenhouse systems.

Table 3
Monitored on-site weather data.

Measures	Sampling interval	Instrument	Accuracy
Dry bulb temperature (°C)	5 min	Hobonet S-THB	±0.2 °C
Relative humidity (%)	5 min	Hobonet S-THB	< ± 5 %
PAR (PPFD)	5 min	Hobonet S-LIA	±5 %
Global horizontal radiation ($W.m^{-2}$)	1 h	Campbell Scientific ClimaVUE50	±5 %
Wind direction (°)	1 h	Campbell Scientific ClimaVUE50	±5°
Wind speed ($m.s^{-1}$)	1 h	Campbell Scientific ClimaVUE50	±3 %
Atmospheric pressure (kPa)	1 h	Campbell Scientific ClimaVUE50	±0.05 kPa
Snow depth (cm)	1 h	Campbell Scientific SR50A	±1 cm

Table 4
Monitored indoor environment conditions and operating variables of the greenhouse.

Measures	Location	Instrument/ Source	Accuracy	Used for calibration
Dry bulb temperature (°C)	Center, 1.5 m above the ground	Hobonet RXW-THC	± 0.2 °C	
Relative humidity (%)	Center, 1.5 m above the ground	Hobonet RXW-THC	< ± 5 %	✔
PAR (PPFD)	NW corner, 3 m above the ground	Hobonet RXW-LIA	± 5 %	
Ground temperature (°C)	Center, 0.1 m underneath the ground	Hobonet RXW-TMB	± 0.2 °C	
Vents actuators status		Local controller		✔
Fans actuactors status		Local controller		✔
Fuel consumption (m^3)		Local controller		✔
Crop yield		Manually registered		

manure treatment, followed by covering the ground with a black tarp. This period does not represent the typical operating conditions of a greenhouse. Consequently, only data collected between September and March are used to complete the calibration of the model.

During that period, the outdoor air temperature fluctuated between −31 °C and 25 °C with an average value of 0.1 °C, while the outdoor air relative humidity was, on average, 79 %. In terms of PAR, it can reach a value of 1690 μmol·$[m^2 \cdot s^{-1}]^{-1}$. The maximum indoor PAR is slightly different between the unheated (716 μmol·$[m^2 \cdot s^{-1}]^{-1}$) and the heated (791 μmol·$[m^2 \cdot s^{-1}]^{-1}$) greenhouses. The difference between the two greenhouses' indoor temperatures is, on average, 1.4 °C when there is no heating or thermal blanket.

3.2. Model creation

An overview of the TRNSYS greenhouse model and the information flow is illustrated in Fig. 4.

The model includes six main components: (1) the weather & operating data; (2) the greenhouse construction; (3) the solar radiation (3D distribution); (4) the infiltration and ventilation (TRNFLOW air network); (5) the ground coupling; and (6) the crop. TRNSYS types or extensions used to simulate these components are listed in Table 5. The components of the TRNSYS model and the initial parameters are detailed in the Supplementary Material.

Table 5
TRNSYS components used in the greenhouse model.

Model component	TRNSYS type or extension	Information specified
Weather & operating data	User specified for model calibration with measured data (Type 9)	5-minutes interval data
Greenhouse construction	· TRNS3d plugin for SketchUp for the geometry Type 56 for construction materials and thermal characteristics	· Orientation Construction properties Windows physical properties Wall boundary conditions
Solar radiation	· Type 16 – Solar processor Type 56 radiation distribution modes	· Perez et al. [39] model for the tilted surface Detailed beam radiation model Detailed diffuse radiation model
Infiltration/ Ventilation	· TRNFLOW air network Type 971 for stages 1–2-3–4 (side vents / side vents + fans 1 & 2) for controls	· Wall averaged wind pressure coefficients Wind velocity profile around the greenhouse Airflow network and link definition
Ground coupling	Type 1224 – Slab on grade	· Soil nodding map Ground thermal properties Far-field and deep-earth boundary conditions Building underground perimeter insulation
Crop	User-defined model [11]	· Geometrical parameters of the cultivated crops Crop biological parameters

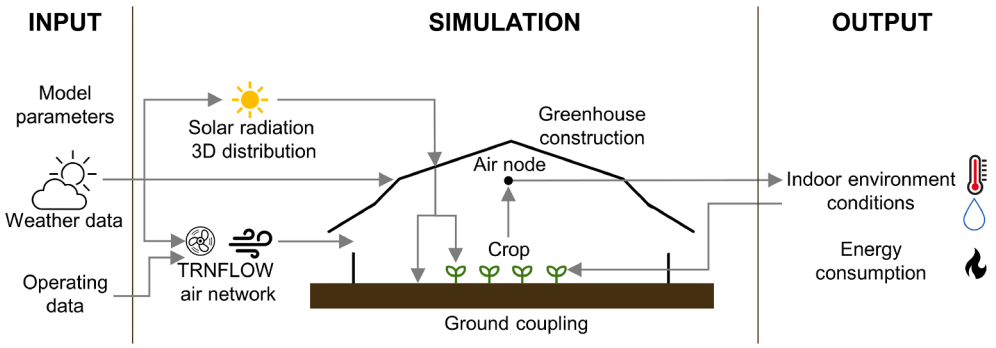

Fig. 4. Simulation overview.

4. Model calibration

The calibration of the greenhouse energy model encompasses several different steps, including the identification of uncertain parameters, a sensitivity analysis to reduce the number of uncertain parameters, and the calibration of the remaining uncertain parameters using the Multi-Objective Genetic Algorithm (MOGA) as described in Sections 4.1–4.3.

4.1. Identification of the model uncertain parameters

Identifying uncertain parameters involves three steps, as described in Section 2.2.1. After the first two steps, a total of 48 uncertain parameters remained. Subsequently, a clustering process is applied to a subset of these parameters, while others that cannot be effectively clustered are used individually. These include building capacitance, the fraction of transmitted solar radiation directly converted to sensible energy (FTSR), and the vents discharge coefficient. Details of the clustering procedures for each uncertain parameter are provided in the following paragraph, resulting in 16 parameters (Table 6) classified as uncertain.

The thermo-chemical properties of the ground (thermal conductivity (λ), heat capacity (Cp), and density (ρ)) are consolidated under "ground diffusivity" (e.g., $\alpha = \frac{\lambda}{\rho \bullet Cp}$). A multiplicative factor is applied as an alternative to modifying the empirical equations for the surface's convection coefficients. Hence, the empirical equations parameters are regrouped under the "convection coefficient factor". For radiometric properties of the greenhouse surfaces, given that the sum of longwave transmissivity (τ), emissivity (ε), and absorptivity (σ) of surfaces equals 1, they are consolidated into a single parameter, "surface longwave radiation (LWR) coefficient". The "surface LWR coefficient" bounds listed in Table 6 pertain to the emissivity of the surface. The values of the other parameters are adjusted proportionally based on their weights. For example, for the initial values $\varepsilon = 0.3$, $\tau = 0.6$ and $\sigma = 0.1$, the weight of τ ($w_\tau = \frac{\tau}{\tau+\sigma}$) is 0.857. Then, for an emissivity of $\varepsilon = 0.4$, $\tau = (1-\varepsilon)\hat{A}\cdot w_\tau = 0.514$ and $\sigma = (1-\varepsilon-\tau) = 0.086$. This approach also applies to shortwave transmissivity, reflectivity (ρ), and absorptivity of the building surfaces (e.g., $\tau + \sigma + \rho = 1$), which are grouped under "surface shortwave radiation (SWR) coefficient". The "SWR coefficient" bounds for polyethylene (PE) and polycarbonate (PC) covers are represented by the transmissivity coefficients. In contrast, the opaque floor surface is defined by the absorptivity coefficient. All relevant parameters used to model the interaction between crops and their environment are grouped under "Crop size" because the equations describing the "big leaf" model (Section A.7 of the Supplementary Material) rely on the heat transfer surface area according to the leaf area index (LAI). All air links' infiltration coefficients and power law exponents are grouped for infiltration flow. The modified parameter for this group is the overall infiltration coefficient, with its bound values shown in Table 6. This adjustment affects the values of all air links infiltration coefficients, as described in section A.6 of the Supplementary Material, while the exponents remain fixed. Finally, for the wind pressure coefficients, all wind pressure coefficients of every wall for all four wind directions (N-S-E-W) are also grouped. For this group, only the values of the windward wind pressure coefficient of each wall are altered, with all others remaining constant.

4.2. Sensitivity analysis

The sensitivity analysis involves calculating global sensitivity indices, as defined by Eq. (1), to provide insight into the contribution and significance of each parameter to the simulated output values during the calibration period, as shown in Fig. 5. A total of 2040 samples are used to compute the global sensitivity indices. This sample size has proven adequate to ensure the sum of the global sensitivity indices nearly equals 1.

Parameters with a global sensitivity index higher than 0.02 for temperature and humidity are identified as sensitive. This choice deviates from the suggested 0.05 value [32] to ensure sufficient parameters for the calibration process. Nine parameters meet the criteria for the temperature sensitivity index and eight for the relative humidity sensitivity index. The eight humidity-sensitive parameters are also temperature-sensitive, as illustrated in Fig. 5. These are building capacitance, ground diffusivity, cover internal convection coefficient, PE LWR coefficient, floor SWR coefficient, PE SWR coefficient, FTSR, crop size (LAI), and vents discharge coefficient.

These parameters are assumed to be constant over time. However, the model uses an average LAI that is associated with the size of each crop. The average LAI varies over time in a greenhouse with irregular or non-uniform crop growth stages. LAI values are calibrated during each calibration stage to account for this variation. As a result, four different LAI values will be calibrated, considering that the first stage consists of two separate weeks.

Fig. 5 shows that the vents discharge coefficient displays the highest sensitivity index for indoor air temperature. This reinforces the assumption of its significant impact and justifies conducting a multi-stage calibration process. The vents discharge coefficient will be calibrated independently in the second calibration stage.

4.3. Calibration of uncertain parameters

Based on the sensitivity analysis, nine parameters have been identified for the multi-stage calibration. The estimation of these parameter

Table 6
Uncertain parameters and bounds.

Calibration period	Parameter	Units	Initial value	Bounds	Step size
Closed vents greenhouse	Building capacitance	$kJ.K^{-1}$	1100	[1100–1900]	100
	Ground diffusivity	$m^2.s^{-1}$	3.5E-7	[1E-7–1E-6]	1E-7
	Cover external convection coefficient factor.	–	1	[0.5–2]	0.1
	Cover internal convection coefficient factor	–	1	[0.5–2]	0.1
	Floor convection coefficient factor	–	1	[0.5–2]	0.1
	Floor LWR coefficient	–	0.90	[0.5–0.96]	0.02
	PE LWR coefficient	–	0.60	[0.5–0.96]	0.02
	PC LWR coefficient	–	0.89	[0.5–0.96]	0.02
	Floor SWR coefficient	–	0.80	[0.6–0.96]	0.02
	PE SWR coefficient	–	0.80	[0.6–0.96]	0.02
	PC SWR coefficient	–	0.76	[0.6–0.96]	0.02
	FTSR	–	0	[0–0.15]	0.01
	Crop size (LAI)	$m^2_{projected}.m^{-2}_{cultivated}$	2.1	[0–6]	0.1
	Infiltration flow coefficient	$kg.s^{-1}$ @1Pa	0.15	[0.05–0.25]	0.01
	Wind pressure coefficient	–	0.70	[0.5–1]	0.02
Ventilated greenhouse	Vents discharge coefficient	–	0.2	[0.1–0.6]	0.01

Legend - PE: Polyethylene; PC: Polycarbonate; LWR: Longwave radiation; SWR: Shortwave radiation; FTSR: Fraction of transmitted solar radiation directly converted to sensible energy; LAI: Leaf area index.

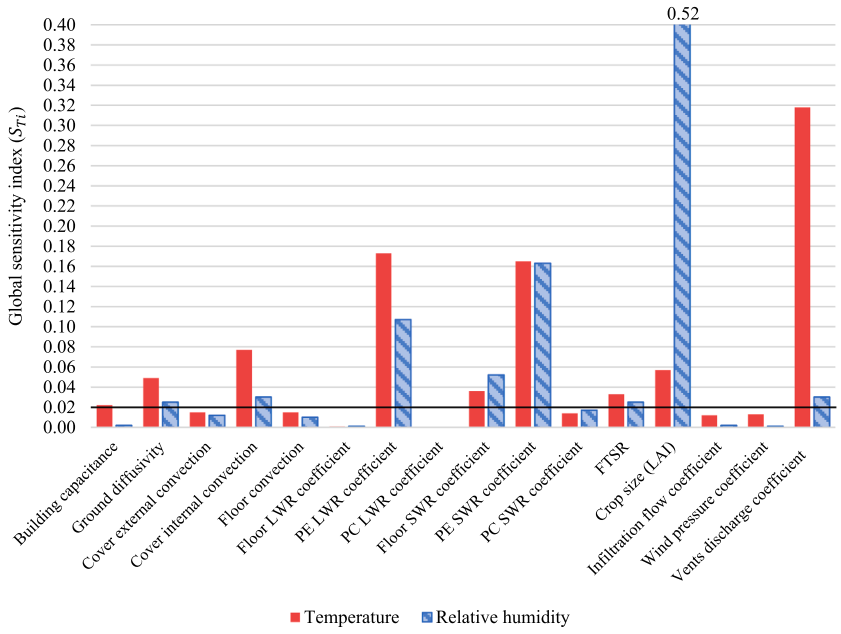

Fig. 5. Global sensitivity indices of identified uncertain parameters.

values is performed using three datasets. It involves the minimization of six objective functions, with three metrics (MAE, RMSE, and MAD) for each variable (T_i and RH_i).

In the first calibration stage, eight uncertain parameters are identified following the sensitivity analysis and are calibrated. However, since the calibration is conducted over two separate weeks where the greenhouse is only ventilated with positive pressure fans, the LAI is calibrated separately for each of the two weeks (November 8th to 15th, 2022 and March 5th to 12th, 2023), resulting in a total of nine parameters to be calibrated. In total, there are more than 8, 000,000,000 possible solutions. The Pareto solutions are obtained after 94 generations with 940 simulations for this first calibration stage. From the Pareto solutions, the Final Optimum Solution (FOS) is for the lower percentage of hours where the error between the simulated and measured indoor air temperature exceeds 1 °C over the calibration period.

Seven parameters are set to their previously calibrated values in the second calibration stage. Only the LAI and the vents discharge coefficient are calibrated during this stage. As explained in previous sections, a new LAI value is calibrated for each period. The model is calibrated from October 10th to 31st, 2022. The Pareto front solutions are obtained after 70 simulations for the second calibration stage since only two parameters are calibrated (1650 possible solutions).

In the third calibration stage, the model includes the control sequence, replacing the previously used input data for the status of the actuators of the vents and fans. The modeling of the opening of the vents and fan operation is described in Section A.6 of the Supplementary Material. The comparison covers the period from September 19th to October 10th, 2022. The only parameter calibrated during this period is the LAI. The calibration process extended over the minimal span of 50 simulations (60 possible solutions).

The calibrated model parameter values from the FOS in all three stages are presented in Table 7. These parameters remained constant throughout the simulation. The LAI values increased from 2.0 to 2.3 between September and October, with a slight decrease to 1.8 in November. According to the greenhouse yield data, this is plausible as most crops are transplanted in September, with a portion harvested in October.

These values appear to be well-distributed within the range, avoiding too many extremes, which confirms the appropriateness of the selected bounds [40]. The discharge coefficient of the vents is at the lower end of its range, suggesting that the insect-proof net mesh size is small and might be clogged.

Table 7
Values of the calibrated uncertain parameters.

Calibration stage	Parameter	Units	Lower bound	Upper bound	Value
1	Building capacitance	$kJ.K^{-1}$	1100	1900	1300
	Ground diffusivity	$m^2.s^{-1}$	1E-7	1E-6	1 E-7
	Cover internal convection coefficient factor	–	0.5	2	1.5
	PE emissivity coefficient	–	0.5	0.96	0.94
	Floor solar absorptivity	–	0.6	0.96	0.72
	PE Solar Transmissivity	–	0.6	0.96	0.80
	Solar-to-air fraction	–	0	0.15	0.04
	LAI (November 2022)	$m^2_{projected}.m^{-2}_{cultivated}$	0	6	1.8
	LAI (March 2023)	$m^2_{projected}.m^{-2}_{cultivated}$	0	6	1.4
2	Vents discharge coefficient	–	0.1	0.6	0.14
	LAI (October 2022)	$m^2_{projected}.m^{-2}_{cultivated}$	0	6	2.3
3	LAI (September 2022)	$m^2_{projected}.m^{-2}_{cultivated}$	0	6	2.0

5. Results

The results obtained following the calibration are first presented, followed by the model validation results.

5.1. Calibration results

The qualitative indoor temperature and relative humidity comparison between measurements and simulation over all three calibration stages are shown in Figs. 6 and 7, respectively.

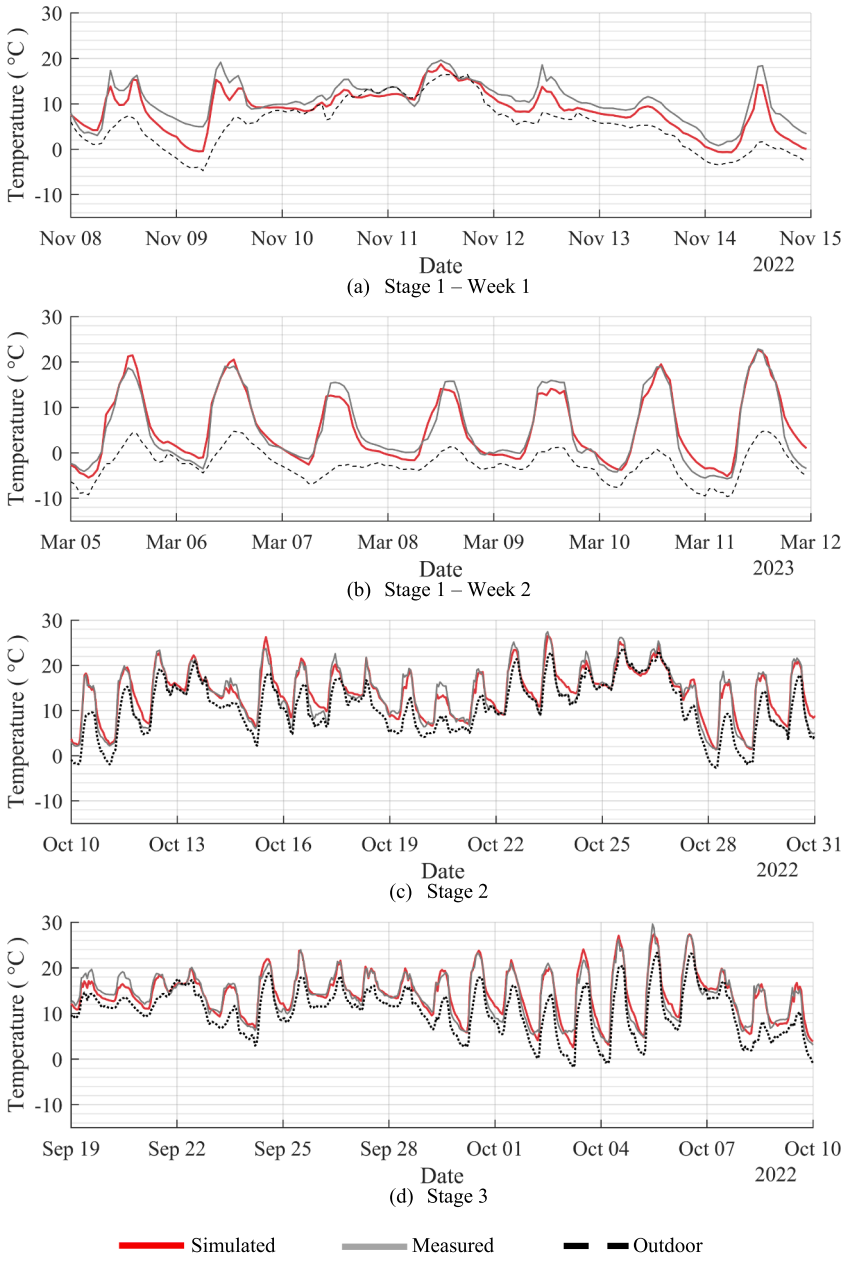

Fig. 6. Comparison of indoor air temperature between measurements and simulation results from (a) calibration stage 1 – Week 1; (b) calibration stage 1 – Week 2; (c) calibration stage 2; and (d) calibration stage 3.

5.1.1. *Indoor air temperature*

The indoor air temperature, measured and simulated throughout all calibration stages, displays a similar pattern in the data most of the time. During the November calibration period, the prevailing overcast conditions led to minimal diurnal temperature fluctuations (Fig. 6(a)). On the contrary, the periods of September (Fig. 6(d)), October (Fig. 6(c) and (d)), and March (Fig. 6(b)) are characterized by sunnier conditions, facilitating the calibration of parameters related to solar radiation. The indoor temperature closely follows the fluctuation in outdoor temperature and global irradiance. There is a variation in overestimating and underestimating the daytime temperatures, indicating that the calibration process strives for equilibrium. The same behavior is observed during nighttime, with predicted temperatures sometimes overestimated and sometimes underestimated. This suggests that it is not just one phenomenon that is not well modeled or omitted but instead arising from various sources of uncertainty, including parameter, model form, and observation uncertainty [15].

5.1.2. *Indoor air relative humidity*

For the relative humidity, Fig. 7 presents the measured and simulated indoor air relative humidity across all the calibration stages, including the range of measurement uncertainty (shaded area). A discernible pattern persists, albeit less evident than the one observed for the indoor air temperature. Fig. 7(a) and (b) reveal disparities, with instances of both overestimation and underestimation. In the operating context of a greenhouse with uncontrollable parameters, predicting the humidity level becomes challenging [4]. During hotter periods when vents are frequently open (September and October), the simulated relative humidity aligns with measured data, as shown in Fig. 7(c) and (d). This follows the pattern of high relative humidity at night, decreasing during the day as the temperatures rise. Also, in Fig. 7(d), the simulated relative humidity is more accurate at the beginning of the period. Towards the end, there is an overestimation of relative humidity, which could be attributed to an overestimation of the LAI, which does not account for crop harvesting. The LAI value represents an average

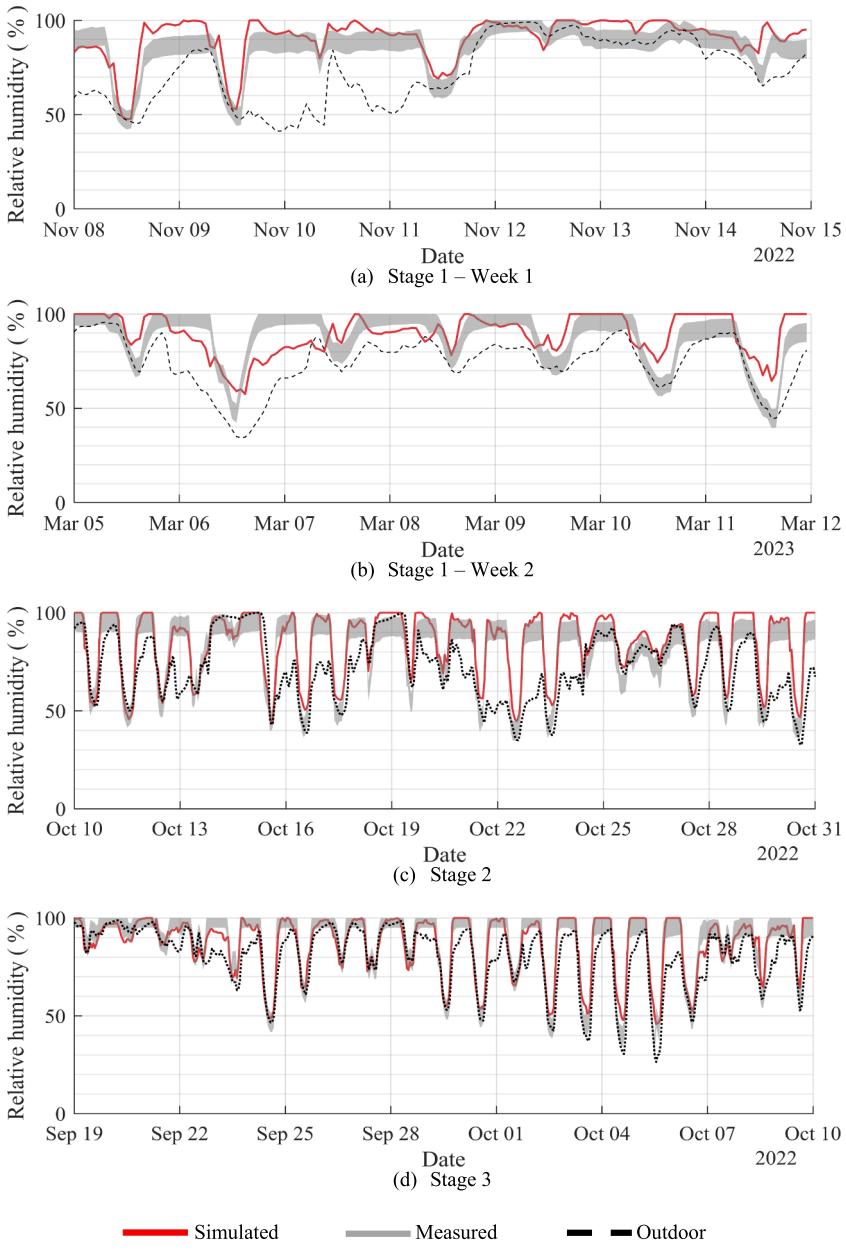

Fig. 7. Comparison of indoor air relative humidity between measurements and simulation results from (a) calibration stage 1 – Week 1; (b) calibration stage 1 – Week 2; (c) calibration stage 2; and (d) calibration stage 3.

value over the entire period, which is a simplification, overlooking crop growth and harvesting processes. According to the greenhouse yield data, this is plausible as most crops are transplanted in September and harvested in October.

5.1.3. *Overview of the multi-stage calibration*

The calibration criteria achieved with each stage FOS are presented in Table 8, providing a detailed breakdown of the performance in each calibration stage and the initial and calibrated model over all periods. The indoor air temperature and relative humidity simulations improved

Table 8
Hourly results for each of the calibration stages.

Calibration stage	Indoor air temperature			Indoor air relative humidity			Selection criteria			
	RMSE (°C)	MBE (°C)	MAD (°C)	RMSE (%)	MBE (%)	MAD (%)	1 °C Error (%)	2 °C Error (%)	5 % Error (%)	10 % Error (%)
Initial model	2.9	1.3	9.8	8.5	−2.7	29.8	48	33	14	4
1	2.2	−0.8	5.4	9.7	3.3	30.2	19	9	44	20
2	1.5	0.4	4.5	7.2	4.4	27.7	29	15	50	9
3	1.3	0.2	3.8	5.1	−1.2	17.0	22	10	9	2
Complete	1.6	−0.01	6.8	8.3	−1.0	44.9	24	13	19	5

from the initial model. The hourly root mean square error (RMSE) over 56 days is reduced from 2.9 °C to 1.6 °C for the indoor temperature while slightly improving from 8.5 % to 8.3 % for the humidity. The predictions of the indoor environment conditions are more accurate in stages 2 and 3, even though most parameters are calibrated during the first stage under different weather conditions and operating modes. This supports effective calibration of the parameters selected in the first and second calibration stages.

Moreover, the increased accuracy of the predicted indoor temperature and relative humidity compared to when the measured status of the actuators is provided confirms the successful implementation of the control sequence. Simulation errors are more critical when the input data forces the vent openings before the simulated temperature reaches the set point.

Additional metrics found in the literature, such as the Coefficient of determination (R^2) (equation (8)), the Coefficient of Variance of the Root Mean Square Error (CV-RMSE), and the Normalized Mean Bias Error (NMBE), are also tabulated (Table 9). Since there are no standardized validation criteria, using these additional metrics enables a comparison of the model's prediction with those of other models in the literature.

$$R^2(-) = 1 - \frac{\sum_{i=1}^{n}(\widehat{y}_i - y_i)^2}{\sum_{i=1}^{n}(\widehat{y}_i - \overline{y}_i)^2} \tag{8}$$

The calibration results meet the recommendation in ASHRAE Guideline 14-2014 [38] for hourly calibration ($R^2 > 0.75$; CV-RMSE < 30 %; NMBE < 10 %), except the R^2 for the indoor air relative humidity during the first stage. Even the normalized metrics for the first calibration stage, where the average temperature of 7.8 °C does not capture the significant temperature variability over the period (min: −5.7 °C and max: 22.9 °C), are within the recommended criteria.

Globally, the results presented in Figs. 6 & 7, and Tables 8 & 9 collectively demonstrate that the multi-stage calibration yielded satisfactory results across all periods for indoor air temperature and relative humidity. These results instill confidence that the calibrated parameters closely reflect real-world conditions and that the model accurately replicates observed thermal behavior. This level of accuracy and confidence justifies advancing to the validation stage.

5.2. Validation results

Following the multi-stage calibration, the calibrated model is validated over two periods: (1) data from the preceding year (2021) for the unheated greenhouse, and (2) data, including the heating consumption, recorded over the whole operating season (October 2022 to March 2023) for the minimally heated greenhouse.

The validation period for the unheated greenhouse spanned 43 days in Autumn 2021, starting at the beginning of the harvest season in September and ending in the final days of October, as the use of thermal blankets typically begins after this period. The crop growth stages are assumed to be similar to those of 2022; hence, the previously calibrated LAI values are used.

Fig. 8 compares the measured and calibrated model prediction of indoor air temperature (a) and the relative humidity (b) for the unheated greenhouse. The results show that the calibrated model has an overall high accuracy. However, discrepancies are observed during specific daytime periods since solar radiation gains influence daytime temperatures. One potential explanation for these discrepancies is that the double polyethylene cover had a higher solar transmissivity coefficient in 2021, which degraded over time, previously observed in harsh weather conditions for polyethylene covers [41] and can annually decline by 2–4 % [42].

For the second validation, using data from the minimally heated twin greenhouse, a 44-kW air heater is added to maintain the indoor air temperature above the setpoints presented in Table 10. Section A.8 of the Supplementary Material details the air heater implementation.

The validation period extended across 162 days of operation (October 2022 to March 2023). The crop growth stages, specified using the LAI, are assumed to be similar to those of the unheated greenhouse. Hence, the previously calibrated LAI values are used. For the periods not included as part of the calibration process, the LAI is fixed at 1.6, the average value over the November and March calibration periods. Fig. 9 compares the measured and calibrated model prediction of (a) the indoor air temperature and (b) the relative humidity for the heated greenhouse for the week where there was a change in the heating set point from 6 °C to 2 °C. As illustrated in Fig. 9 (a), the indoor air temperature closely follows the heating set point during nighttime. Fig. 9 (b) shows that the model overestimates the indoor relative humidity during daytime periods. This discrepancy might be explained by the fixed LAI value used.

Table 11 presents the statistical metrics for the calibrated greenhouse model, calculated using the complete calibration dataset, and for both validation periods, including the heating consumption for the second validation. The values for the initial models are those for the heated greenhouse from October 1st, 2022, to March 1st, 2023. Monthly heating consumption data are aggregated using a weather normalization technique and manually recorded measurements taken over irregular periods [43]. The heating consumption represents the amount of energy the air unit heater provides to maintain the required temperature in the greenhouse.The calibration improved the simulated indoor air temperatures while ensuring the indoor relative humidity remained acceptable. For both validation periods, the RMSE over the indoor air temperature and relative humidity closely match reported data in the literature [7]. The results show a RMSE below 2 °C for temperature and below 10 % for relative humidity. However, a direct comparison may not be representative due to disparities in validation periods and metrics. The metrics of calibrated value are similar to those obtained for the unheated and heated greenhouses, demonstrating the validity of the model. The indoor air relative humidity remains at the same acceptable accuracy level, close to the measurement accuracy of the sensor of 5 %; natural ventilation in the greenhouse results in the indoor humidity mirroring the outdoor levels.

When comparing monthly heating consumption, the results are under the recommended range by ASHRAE Guideline 14–2014 [38]. The yearly measured and simulated heating consumption are 37.6 GJ and 38.9 GJ, respectively, which implies a relative error of +3.7 %. Fig. 10 shows the monthly heating consumption of the initial and

Table 9
Additional hourly statistical metrics for each of the calibration stages.

Calibration stage	Indoor air temperature (°C)				Indoor air relative humidity (%)			
	Stage average	CV-RMSE (%)	NMBE (%)	R^2 (–)	Stage average	CV-RMSE (%)	NMBE (%)	R^2 (–)
Initial model	12.3 °C	23.9	11.0	0.64	85.7 %	9.9	−3.2	0.68
1	7.8 °C	28.1	−10.7	0.88	86.8 %	11.2	3.8	0.24
2	13.5 °C	11.4	2.7	0.92	80.3 %	8.9	5.5	0.81
3	14.1 °C	9.0	1.1	0.94	88.1 %	5.7	−1.4	0.88
Complete	12.3 °C	13.2	−0.01	0.92	85.7 %	9.7	−1.2	0.76

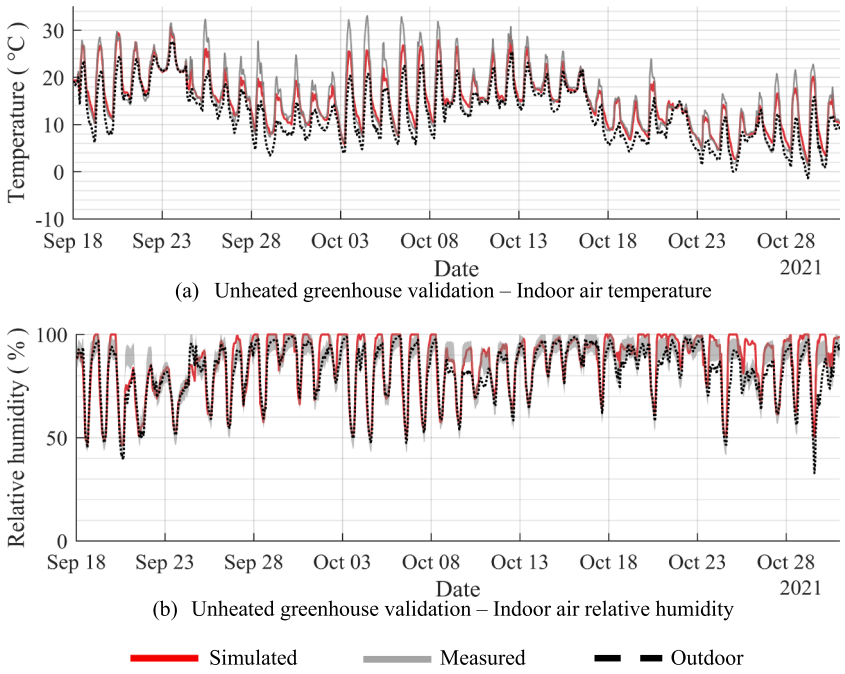

Fig. 8. Comparison of indoor air (a) temperature and (b) relative humidity between measurements and simulation results of the unheated greenhouse in 2021.

Table 10
Heating setpoints during the heated greenhouse validation period.

Sequence	Heating period	Setpoint
1	October 1st to November 21st	6 °C
2	November 21st to February 28th	2 °C

calibrated model compared with the measured data. The calibrated model leads to good results in November and December, but the heating consumption is underestimated by 23 % in October and overestimated by 10 % in January and February. Ideally, the relative errors in monthly heating consumption should remain below 10 %. However, the simulation results effectively capture the subtle distinctions in monthly heating consumption between January and February (a 3 % gap), thereby reinforcing confidence in the trends observed in the obtained results. Furthermore, the observed variation in October is likely attributed to low heating demands, with the system operating only 10 days throughout the month. A slight temperature overestimation during this period can potentially prevent the heating system from turning on.

The calibration improved the predictions for the heating consumption. However, the initial model, which used parameters from the literature, appeared to underestimate the greenhouse's heat loss,

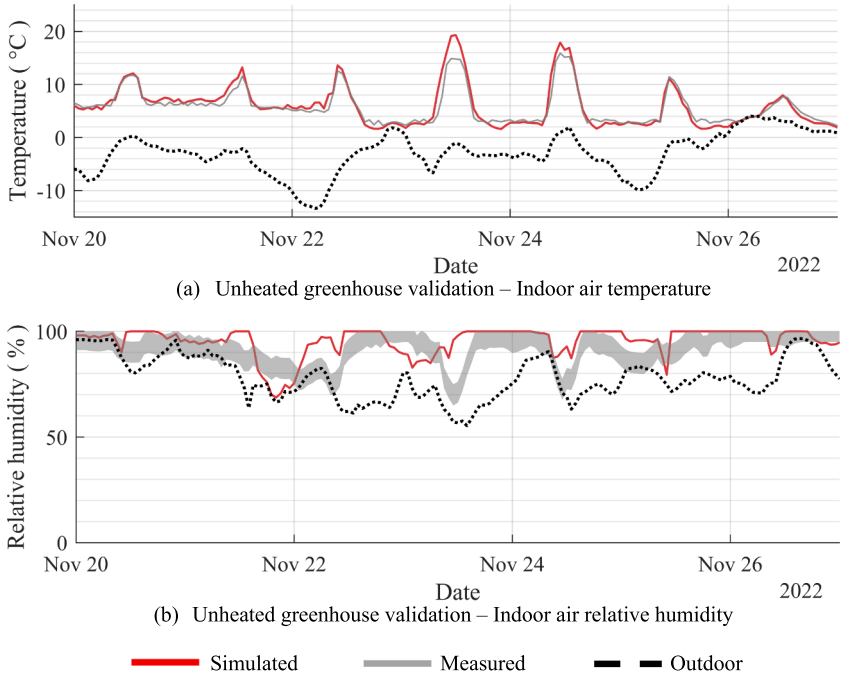

Fig. 9. Comparison of indoor air (a) temperature and (b) relative humidity between measurements and simulation results of the heated greenhouse for the week of 20 to 27 November 2022.

Table 11
Results of the validation of the greenhouse model.

Validation data	Indoor air temperature			Indoor air relative humidity			Heating consumption	
	RMSE (°C)	MBE (°C)	1 °C Error (%)	RMSE (%)	MBE (%)	5 % Error (%)	NMBE (%)	CV-RMSE (%)
Initial model	2.4	1.5	48	7.3	2.2	30	−18.6	20.0
Calibrated	1.6	−0.01	24	8.3	−1.0	19	–	–
Unheated	1.8	−0.5	18	5.3	1.5	18	–	–
Heated	1.9	0.5	29	8.4	3.4	32	3.7	9.3

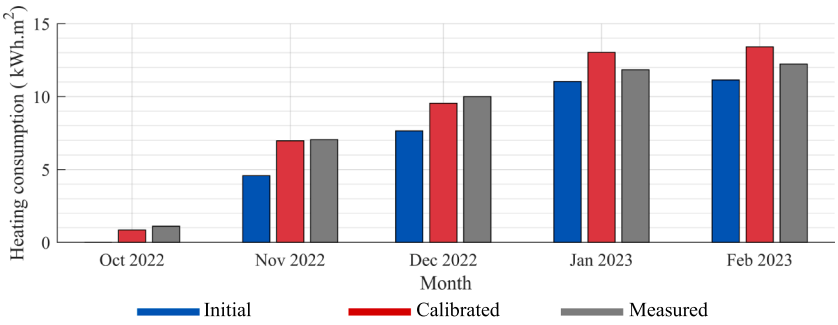

Fig. 10. Comparison of heating consumption between measurements and simulation results of the minimally heated greenhouse.

resulting in lower heating consumption throughout all months, particularly in October, November, and December.

Ultimately, the statistical metrics and the trend comparison bolster confidence in the model's applicability for future years under weather conditions like those prevailing during the validation process.

6. Discussion

This study aims to develop a small-scale greenhouse energy model using TRNSYS to provide reliable predictions for greenhouse indoor environment conditions and energy consumption to support future analysis. The model closely predicts the unheated and heated indoor environment conditions of the greenhouse. The RMSE of air temperature is lower than 2 °C, and the RMSE of relative humidity is lower than 10 %. These values are within the range of most greenhouse models [7]. Regarding heating consumption for the heated greenhouse, the monthly NMBE in model predictions (+3.7 %) is small, demonstrating that the model captures the heating profile, even in a minimally heated greenhouse. The monthly heating consumption accuracy is below the recommended levels in building performance simulation [38].

The predictions of heating consumption could be further improved. The validation results are inconsistent compared to the calibration results. There appears to be a misrepresentation of thermal interaction within the greenhouse during January and February. The presence of snow could explain this difference as it acts as an insulator for the bottom of the greenhouse, decreasing heat loss and infiltration. The conditions during the first calibration stage resemble those of the heating season, with lower temperatures and closed ventilation vents. However, extremely cold temperatures, limited sunlight hours, and substantial snowfall, characteristic of the winter in this area, are not accounted for. It suggests that the model might need to be calibrated over a typical winter period to identify more representative constant parameter values for all seasons. The lack of data during free-floating winter periods contributed to the observed overestimation. Maintaining constant parameters throughout all seasons may not accurately reflect the dynamic nature of the system. It may be necessary to incorporate weather-dependent equations to adjust model parameters for improved representation.

The model also exhibits a systematic error in simulating relative humidity. The observed discrepancy in simulated relative humidity compared to measured values could be attributed to the crop modeling approach. The crop model was initially developed for lettuce crops using data from plant factory conditions [44]. Therefore, its application under cold conditions, such as during nights with temperatures below 0 °C (March 6th to 7th), might not be appropriate, as it is used outside the conditions for which it was initially designed. It is worth noting that chilling injury from cold temperatures tends to affect the biological activity of crops [45]. Furthermore, the model parameter values are based on the lettuce experiments, potentially not accurately representing the diverse varieties of leafy greens cultivated in the greenhouse. The crop model should be validated over a broader range of indoor environment conditions and crop variety. Despite accounting for the limitations inherent to the model development, the crop model performs effectively when combined with a calibration process.

Compared to other greenhouse validation studies, the datasets used in this study are relatively long, lasting 43 days and 162 days. Ideally, validating a greenhouse energy model for annual energy analysis requires a complete year of data. However, reviews by Katzin et al. [7] and Beaulac et al. [9] revealed that greenhouse model validations often use considerably smaller datasets. Through extensive validation, various discrepancies in the model where identified, highlighting the importance of an extended validation period that may uncover issues not apparent in a shorter timeframe. This suggests that short validation periods can show that the model is valid, even with discrepancies. It emphasizes that the model performances may vary across weather conditions and operating modes. The observed differences in simulated and measured heating consumption show the importance of having precise knowledge of the activities occurring within a greenhouse.

One of the strengths of the study lies in the data used, which are sourced from a typical small-scale greenhouse in commercial operation. Katzin et al. [7] and Beaulac et al. [9] reviews also indicated that greenhouse model validations frequently rely on experimental greenhouse and research compartments data instead of commercially operated greenhouses. The validation based on non-commercially operated greenhouses does not guarantee that the model will be applicable for assessing the performance of commercial greenhouses, including the associated operation uncertainties. In an operating greenhouse, in contrast to an experimental one where all operations are closely monitored, having a comprehensive understanding of ongoing operations is crucial.

Nevertheless, despite the extensive validation conducted in this paper compared to existing literature, it relies on data measured at a

single site and with numerous parameters that had to be estimated and could not be directly measured. Using data from multiple greenhouses in different weather conditions and conducting a validation over an entire year could be used to evaluate further and improve the TRNSYS model. Extensive validation assures that the calibration does not merely compensate for modeling errors.

The proposed calibration method attained satisfactory model predictions, as reported results showed. The approach is time-consuming but proves worthwhile when applied to a typical greenhouse format that can be replicated and used for further analyses. In terms of computational power requirements, the sensitivity analysis demonstrated its effectiveness in reducing the number of parameters that needed adjustment, resulting in a smaller optimization domain, with the potential for the 8 ,000 ,000 ,000 possibilities to be even higher. Nevertheless, the calibration time could be optimized by selecting a higher sensitivity index criterion to include fewer sensitive parameters without affecting the results.

The current calibration processes are typically ad-hoc, involving multiple manual iterations with user intervention based on expert judgment, lacking a well-defined, data-driven procedure. However, some literature studies have proposed methods for addressing calibration issues. The proposed calibration method is well-detailed in this paper and replicable in other studies. While obtaining data for multi-stage calibration is not always feasible, single-stage MOGA is still recommended.

Finally, key attributes of the model are its replicability and that it is developed in TRNSYS, where an important library of components is available, enabling the integration of various HVAC and renewable energy systems. Including all the detailed modeling approaches available in TRNSYS and a crop hygrothermal interactions model, the model presents the current state-of-the-art practices in greenhouse energy modeling.

7. Conclusions

Considering the lack of extensively validated greenhouse energy models, this paper attempts to develop a detailed model using TRNSYS. The model included detailed energy modeling components available in TRNSYS and integrated a hygrothermal crop model. The TRNFLOW infiltration sub-model introduced a novel approach based on an on-site air leakage test. A sensitivity analysis was conducted to identify sensible parameters, followed by a multi-stage automated calibration method to calibrate the model's uncertain parameters. The validation process was then conducted using two additional datasets to assess the applicability of the calibrated model.

The case study was a typical small-scale ventilated greenhouse in Victoriaville, Canada. The comparison between the simulated and measured data during the multi-stage calibration process indicated that the model accurately replicated measured experimental conditions when the model parameters were adjusted to fit those indoor environment conditions. Using the calibrated parameters, the greenhouse energy model provided the same insight into the greenhouse environment conditions for the previous year in the same weather conditions. When assessing the model with data from a minimally heated twin greenhouse, the yearly heating consumption resulted in a relative error of 3.7 %.

With this multi-purpose model, whose predictive capacity has been validated, numerous opportunities exist, such as analyzing various scenarios for energy efficiency measures, renewable energy technologies, control algorithms, seeding schedules, subsidy applications, environmental policies, and regulations. The model can also study various performance metrics, including indoor environment conditions, energy consumption, carbon footprint, crop production, and operating costs. In a way, this project is a springboard to various possibilities aimed at developing greenhouse farming. In future studies, a plant growth model will be integrated to measure the productivity of the greenhouse and the influence of plant growth on energy consumption.

CRediT authorship contribution statement

Arnaud Beaulac: Writing – original draft, Formal analysis, Methodology, Validation. **Timothé Lalonde:** Writing – original draft, Investigation, Formal analysis, Conceptualization. **Didier Haillot:** Writing – review & editing, Supervision, Methodology, Funding acquisition, Conceptualization. **Danielle Monfet:** Writing – review & editing, Supervision, Methodology, Funding acquisition, Conceptualization.

Declaration of competing interest

The authors declare that they have no known competing financial interests or personal relationships that could have appeared to influence the work reported in this paper.

Data availability

The authors do not have permission to share data.

Acknowledgments

Part of the project was supported by the Natural Sciences and Engineering Research Council of Canada (NSERC) Alliance grants ALLRP 561361-21 and the Réseau québécois de l'énergie intelligente (RQEI), a strategic cluster funded by Quebec Research Fund Nature and Technology. We want to offer our special thanks to CÉTAB + for their precious collaboration and sharing of experimental data.

Appendix A. Supplementary data

Supplementary data to this article can be found online at https://doi.org/10.1016/j.applthermaleng.2024.123195.

References

[1] J. Eaves, S. Eaves, Comparing the profitability of a greenhouse to a vertical farm in Quebec, Can. J. Agric. Econ./Rev. Canadien. D'agroecon. 66 (2018) 43–54, https://doi.org/10.1111/cjag.12161.
[2] E. Runkle, A.J. Both, Greenhouse Energy Conservation Strategies, 2011, doi: 10.7282/T3K64KWN.
[3] M.-H. Talbot, T. Lalonde, A. Beaulac, D. Haillot, D. Monfet, Comparing the energy performance of different controlled environment agriculture spaces using TRNSYS. vol. 12, IBPSA-Canada; 2022, p. 0–0.
[4] X. Zhou, Q. Liu, D. Katzin, T. Qian, E. Heuvelink, L.F.M. Marcelis, Boosting the prediction accuracy of a process-based greenhouse climate-tomato production model by particle filtering and deep learning, Comput. Electron. Agric. 211 (2023) 107980, https://doi.org/10.1016/j.compag.2023.107980.
[5] M.N. Heyat Jilani, S. Yadav, C. Hachem-Vermette, S. Panda, G. Tiwari, S. Nayak, Design and performance evaluation of a greenhouse integrated Thin-Film Photovoltaic system and an earth air heat exchanger, Appl. Therm. Eng. 231 (2023), https://doi.org/10.1016/j.applthermaleng.2023.120856.
[6] J. Xiao, Q. Wang, X. Wang, Y. Hu, Y. Cao, J. Li, An earth-air heat exchanger integrated with a greenhouse in cold-winter and hot-summer regions of northern China: modeling and experimental analysis, Appl. Therm. Eng. 232 (2023) 120939, https://doi.org/10.1016/j.applthermaleng.2023.120939.
[7] D. Katzin, E.J. van Henten, S. van Mourik, Process-based greenhouse climate models: genealogy, current status, and future directions, Agr. Syst. 198 (2022) 103388, https://doi.org/10.1016/j.agsy.2022.103388.
[8] S.A. Klein, W.A. Beckamn, J.W. Mitchell, J.A. Duffie, N.A. Duffie, J.C. Mitchell et al., TRNSYS 18: A transient system simulation program 2017 Solar Energy Laboratory, University of Wisconsin. Wisconsin, USA, USA.
[9] A. Beaulac, D. Monfet, D. Haillot, Revue de la modélisation énergétique de serres avec TRNSYS. vol. 1, Reims, France: 2023, p. 69–76. doi: 10.25855/SFT2023-064.
[10] M.S. Ahamed, H. Guo, K. Tanino, Modeling heating demands in a Chinese-style solar greenhouse using the transient building energy simulation model TRNSYS, J. Build. Eng. 29 (2020) 101114, https://doi.org/10.1016/j.jobe.2019.101114.
[11] M.-H. Talbot, D. Monfet, Estimating the impact of crops on peak loads of a Building-Integrated Agriculture space, Sci. Technol. Built Environ. 26 (2020) 1448–1460, https://doi.org/10.1080/23744731.2020.1806594.
[12] C. Lavigueur, Improving Greenhouse Modelling in Building Performance Simulation Tools, Mémoire, Polytechnique Montréal, 2022.
[13] Sansregret S, Lavigne K. Lessons Learned from the Calibration of 5 Building Models with Total Electric Demand Measurement on 15-Minutes Intervals. vol. 14, IBPSA; 2015, p. 2889–96. doi: 10.26868/25222708.2015.2465.

[14] D. Coakley, P. Raftery, M. Keane, A review of methods to match building energy simulation models to measured data, Renew. Sust. Energy Rev. 37 (2014) 123–141, https://doi.org/10.1016/j.rser.2014.05.007.
[15] A. Chong, Y. Gu, H. Jia, Calibrating building energy simulation models: A review of the basics to guide future work, Energ. Buildings 253 (2021) 111533, https://doi.org/10.1016/j.enbuild.2021.111533.
[16] M.A. Adesanya, W.-H. Na, A. Rabiu, Q.O. Ogunlowo, T.D. Akpenpuun, A. Rasheed, et al., TRNSYS simulation and experimental validation of internal temperature and heating demand in a glass greenhouse, Sustainability 14 (2022) 8283, https://doi.org/10.3390/su14148283.
[17] C. Baglivo, D. Mazzeo, S. Panico, S. Bonuso, N. Matera, P.M. Congedo, et al., Complete greenhouse dynamic simulation tool to assess the crop thermal well-being and energy needs, Appl. Therm. Eng. 179 (2020) 115698, https://doi.org/10.1016/j.applthermaleng.2020.115698.
[18] Q.O. Ogunlowo, W.H. Na, A. Rabiu, M.A. Adesanya, T.D. Akpenpuun, H.T. Kim, et al., Effect of envelope characteristics on the accuracy of discretized greenhouse model in TRNSYS, J. Agric. Eng. (2022), https://doi.org/10.4081/jae.2022.1420.
[19] A. Rasheed, J.W. Lee, H.W. Lee, Development and optimization of a building energy simulation model to study the effect of greenhouse design parameters, Energies 11 (2018) 2001, https://doi.org/10.3390/en11082001.
[20] U.-H. Yeo, S.-Y. Lee, S.-J. Park, J.-G. Kim, Y.-B. Choi, R.-W. Kim, et al., Rooftop greenhouse: (1) design and validation of a BES model for a plastic-covered greenhouse considering the tomato crop model and natural ventilation characteristics, Agriculture 12 (2022) 903, https://doi.org/10.3390/agriculture12070903.
[21] J. Chen, J. Yang, J. Zhao, F. Xu, Z. Shen, L. Zhang, Energy demand forecasting of the greenhouses using nonlinear models based on model optimized prediction method, Neurocomputing 174 (2016) 1087–1100, https://doi.org/10.1016/j.neucom.2015.09.105.
[22] E. Cruz-Valeriano, O. Begovich, J. Ruiz-León, Modeling of a greenhouse using Particle Swarm Optimization, in: 2013 10th International Conference on Electrical Engineering, Computing Science and Automatic Control (CCE), 2013, pp. 268–273, https://doi.org/10.1109/ICEEE.2013.6676034.
[23] A. Hasni, R. Taibi, B. Draoui, T. Boulard, Optimization of greenhouse climate model parameters using particle swarm optimization and genetic algorithms, Energy Proc. 6 (2011) 371–380, https://doi.org/10.1016/j.egypro.2011.05.043.
[24] A. Pérez-González, O. Begovich-Mendoza, J. Ruiz-León, Modeling of a greenhouse prototype using PSO and differential evolution algorithms based on a real-time LabView^{TM} application, Appl. Soft Comput. 62 (2018) 86–100, https://doi.org/10.1016/j.asoc.2017.10.023.
[25] H. Yang, Q.-F. Liu, H.-Q. Yang, Deterministic and stochastic modelling of greenhouse microclimate, Syst. Sci. Control Eng. 7 (2019) 65–72, https://doi.org/10.1080/21642583.2019.1661310.
[26] J.M. Herrero, X. Blasco, M. Martínez, C. Ramos, J. Sanchis, Robust identification of non-linear greenhouse model using evolutionary algorithms, Control Eng. Pract. 16 (2008) 515–530, https://doi.org/10.1016/j.conengprac.2007.06.001.
[27] K. Lammarï, F. Bounaama, B. Ouradj, B. Draouï, Constrained GA PI sliding mode control of indoor climate coupled mimo greenhouse model, J. Therm. Eng. 6 (2020) 313–326, https://doi.org/10.18186/thermal.711554.
[28] R. Guzmán-Cruz, R. Castañeda-Miranda, J.J. García-Escalante, I.L. López-Cruz, A. Lara-Herrera, J.I. de la Rosa, Calibration of a greenhouse climate model using evolutionary algorithms, Biosyst. Eng. 104 (2009) 135–142, https://doi.org/10.1016/j.biosystemseng.2009.06.006.
[29] R. Ward R. Choudhary C. Cundy G. Johnson A. McRobie, Simulation of plants in buildings; incorporating plant-air interactions in building energy simulation, in: 14th International Conference of IBPSA-Building Simulation 2015, BS 2015, Conference Proceedings, 2015, p. 2256–63.
[30] D.B. Crawley, J.W. Hand, M. Kummert, B.T. Griffith, Contrasting the capabilities of building energy performance simulation programs, Build. Environ. 43 (2008) 661–673, https://doi.org/10.1016/j.buildenv.2006.10.027.
[31] P. Raftery, M. Keane, J. O'Donnell, Calibrating whole building energy models: an evidence-based methodology, Energ. Build. 43 (2011) 2356–2364, https://doi.org/10.1016/j.enbuild.2011.05.020.
[32] F.M. Baba, H. Ge, R. Zmeureanu, L. Wang, Calibration of building model based on indoor temperature for overheating assessment using genetic algorithm: methodology, evaluation criteria, and case study, Build. Environ. 207 (2022) 108518, https://doi.org/10.1016/j.buildenv.2021.108518.
[33] J.L. Hatfield, J.H. Prueger, Temperature extremes: effect on plant growth and development, Weather Clim. Extremes 10 (2015) 4–10, https://doi.org/10.1016/j.wace.2015.08.001.
[34] W. Tian, A review of sensitivity analysis methods in building energy analysis, Renew. Sustain. Energy Rev. 20 (2013) 411–419, https://doi.org/10.1016/j.rser.2012.12.014.
[35] I.M. Sobol′, Global sensitivity indices for nonlinear mathematical models and their Monte Carlo estimates, Math. Comput. Simul 55 (2001) 271–280, https://doi.org/10.1016/S0378-4754(00)00270-6.
[36] A. Saltelli, P. Annoni, I. Azzini, F. Campolongo, M. Ratto, S. Tarantola, Variance based sensitivity analysis of model output. design and estimator for the total sensitivity index, Comput. Phys. Commun. 181 (2010) 259–270, https://doi.org/10.1016/j.cpc.2009.09.018.
[37] H. Li, Y. Li, X. Yue, X. Liu, S. Tian, T. Li, Evaluation of airflow pattern and thermal behavior of the arched greenhouses with designed roof ventilation scenarios using CFD simulation, PLoS One 15 (2020) e0239851.
[38] ASHRAE. Guideline 14-2014, Measurement of energy and demand savings. Atlanta, Georgia, USA: American Society of Heating, Ventilating, and Air Conditioning Engineers, 2014.
[39] R. Perez, P. Ineichen, R. Seals, J. Michalsky, R. Stewart, Modeling daylight availability and irradiance components from direct and global irradiance, Sol. Energy 44 (1990) 271–289, https://doi.org/10.1016/0038-092X(90)90055-H.
[40] M.J. Ten, strategies towards successful calibration of environmental models, J. Hydrol. 620 (2023) 129414, https://doi.org/10.1016/j.jhydrol.2023.129414.
[41] I. Al-Helal, P. Picuno, A.A. Alsadon, A. Ibrahim, M. Shady, A.M. Abdel-Ghany, Effect of shape, orientation and aging of a plastic greenhouse cover on the degradation rate of the optical properties in arid climates, Appl. Sci. 12 (2022) 2709, https://doi.org/10.3390/app12052709.
[42] J. Nijskens, J. Deltour, E. Albrecht, J. Gratraud, P. Feuilloley, Comparative studies on the ageing of polyethylene film in the laboratory and in practical use, Plasticulture (1990) 11–20.
[43] J.H. Eto, A Comparison of Weather Normalization Techniques for Commercial Building Energy Use, Lawrence Berkeley Laboratory, University of California, Berkeley, CA, 1985.
[44] L. Graamans, A. van den Dobbelsteen, E. Meinen, C. Stanghellini, Plant factories; crop transpiration and energy balance, Agr. Syst. 153 (2017) 138–147, https://doi.org/10.1016/j.agsy.2017.01.003.
[45] L.L. Morris, Chilling injury of horticultural crops: an overview, HortSci. 17 (1982) 161–162, https://doi.org/10.21273/HORTSCI.17.2.161.